

Online Parameter Estimation for Wireless Power Transfer Systems Using the Tangent of the Reflected Impedance Angle

Shufan Li^{*,**}, Chenglin Liao[†], and Lifang Wang^{*,***}

^{†,*}Key Lab. of Power Electron. and Electr. Drive, Inst. of Electrical Eng., Chinese Academy of Sciences, Beijing, China

^{**}University of Chinese Academy of Sciences, Beijing, China

^{***}Collaborative Innovation Center for Electric Vehicles in Beijing, Beijing, China

Abstract

An online estimation method for wireless power transfer (WPT) systems is presented without using any measurement of the secondary side or the load. This parameter estimation method can be applied with a controlling strategy that removes both the receiving terminal controller and the wireless communication. This improves the reliability of the system while reducing its costs and size. In a wireless power transfer system with an LCCL impedance matching circuit under a rectifier load, the actual load value, voltage/current and mutual inductance can be reflected through reflected impedance measuring at the primary side. The proposed method can calculate the phase angle tangent value of the secondary loop circuit impedance via the reflected impedance, which is unrelated to the mutual inductance. Then the load value can be determined based on the relationships between the load value and the secondary loop impedance. After that, the mutual inductance and transfer efficiency can be computed. According to the primary side voltage and current, the load voltage and current can also be detected in real-time. Experiments have verified that high estimation accuracy can be achieved with the proposed method. A single-controller based on the proposed parameter estimation method is established to achieve constant current control over a WPT system.

Key words: Online estimation, Tangent of reflected impedance angle, Reflected impedance, Wireless power transfer system

I. INTRODUCTION

Wireless power transfer technology has been rapidly developed and applied in a wide variety of industrial and consumer applications [1]-[7] due to its advantages in terms of safety, convenience, low maintenance and reliability.

A typical wireless power transfer system generally comprises two parts, namely a transmitting terminal and a receiving terminal, as shown in Fig.1. Power is transferred by two resonant coils based on the magnetic resonant coupling theory [8]. There are impedance compensation circuits on both

the primary and the secondary sides of the coils, improving the power transfer capability of the system [9].

A major issue involved in the study of the WPT systems is parameter variations, along with the difficulties they bring to the control of the whole system. Some studies have been done for the power transfer control of WPT systems [10]-[25]. The authors of [10], [11] tried to control the power flow of a system by changing its circuit topology, while the authors of [12] proposed a method for controlling output current of the DC-AC inverter in response to load changes. Load conditions were monitored and transferred by a wireless communication system for feedback control in [13]-[15].

To ensure the high efficiency and stability of power transfer, a typical wireless power transfer system usually contains controllers on both the transmitting terminal and the receiving terminal. The charging information is collected by the receiving terminal controller and sent to the transmitting terminal by wireless communication technology, and the

Manuscript received Aug. 29, 2016; accepted Aug. 8, 2017

Recommended for publication by Associate Editor Jung-Wook Roh.

[†]Corresponding Author: liaocl@mail.iee.ac.cn

Tel: +86-8254-7088, Inst. of Electrical Eng., Chinese Academy of Sci.

^{*}Key Laboratory of Power Electronics and Electric Drive, Institute of Electrical Engineering, Chinese Academy of Sciences, China

^{**}University of Chinese Academy of Sciences, China

^{***}Collaborative Innovation Center for Electr. Vehicles in Beijing, China

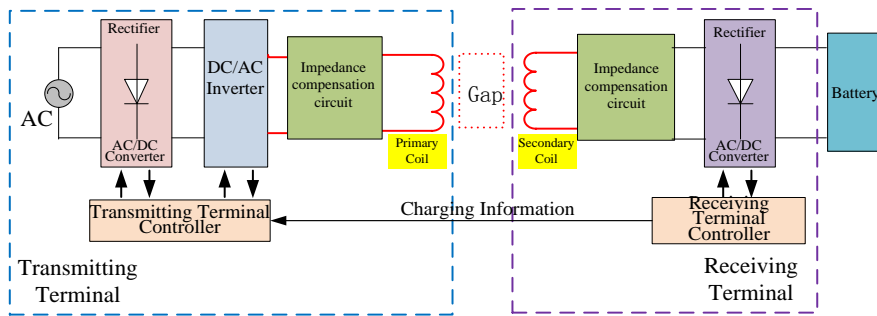


Fig. 1. Structure diagram of a wireless power transfer system.

transmitting terminal controller controls the input voltage and current according to the information it received [16]-[18]. There are limitations of this type of two-controller mode. The first of these limitations is the unreliability of the information transmission. Due to the existence of a magnetic field, the wireless transmission speed is low and the bit error rate is high, reducing the reliability and stability of the system [17]. The second limitation is excess complexity. Both the receiving terminal controller and the wireless communication device can increase the costs and size of the system [19], [20].

To avoid such limits, controlling methods based on a single-controller model have been researched recently [21], [22]. With such methods, information on the primary side instead of the receiving terminal is collected. Then the equivalent load and charging current are estimated, providing controlling information for the single controller on the primary side. This controlling strategy removes both the receiving terminal controller and the wireless communication, improving the reliability of the system while reducing its costs and size. The key to this control strategy is the real-time estimation of the load parameters needed for the controlling. Recently, some studies have focused on the estimation of the load parameters of WPT systems [22]-[25]. In [22], the output voltage of the IPT (Inductive Power Transfer) system is estimated by calculating the track voltage of the primary side. In addition, a phase error that can be used in controlling the track current is estimated by comparing the estimated output voltage and the reference (V_{ref}), which represents the required output voltage. However, this estimation method was based on the assumption of an ideal resonant circuit. Therefore, the estimation errors may increase when the system is put into practical use. Wang et al. [23], [24] sampled the peak value of the primary resonant current by controlling the switches of the IGBTs in a voltage-fed IPT system, and estimated the equivalent resistance load by analyzing the energy transfer procedure. Both simulation and experimental results verified the theory that the heavier the load, the faster the drop rates of the primary resonant current. This estimation method is limited to an IPT system for kitchen appliances, and it is only suitable for voltage-fed systems. Experiments have shown that the accuracy of this load detection method is more than 85%. Yin et al. [25] built a mathematical model of an n-Coil wireless

power transfer system, and estimated the load impedance, output voltage, output current, output power and loop currents by measuring the input voltage and current. This method was verified with a wireless power domino-resonator system consisting eight coil resonators. Despite the high accuracy of this load estimation method, it is only based on the a WPT system under ideal condition.

Another important parameter for the single-controller strategy is the mutual inductance of the coils. The mutual inductance may change due to a lateral misalignment of the coils, a vertical distance change of two coils, or a change of the coils parameters. Once the mutual inductance changes, the power transfer efficiency is affected and the accuracy of the parameter estimation is damaged. Recently, some studies have been done to research changes in the mutual inductance of coils. In [26], the high-misalignment condition is taken into consideration when designing a compensation topology. Takehiro Imura et al. calculated the mutual inductance with a Neumann formula and demonstrated that it matched well with electromagnetic field analysis results [27]. In [28], a formula is established to calculate the mutual inductance of a movable planar coil and a fixed planar coil on a wireless battery charging platform. However, to precisely control the WPT system, the mutual inductance of the coils should be monitored in real time.

To apply a single-controller strategy in a WPT system, an online parameter estimation method is needed to provide accurate information on the load as well as the mutual inductance of the coils. This paper presents an online parameter estimation method satisfying the above needs of a single-controller without the using information from the secondary side or the load. In addition, with the introduction of the tangent value of the reflected impedance angle λ , the proposed parameter estimation method avoids the influence of coils misalignment in the load estimation, and measures the extent of the coils misalignment by calculating the mutual inductance.

II. BASIC ANALYSIS OF A WIRELESS POWER TRANSFER SYSTEM

A. Basic Circuit Topology

In a typical wireless power transfer system, there is always a high frequency inverter, primary coil, secondary coil,

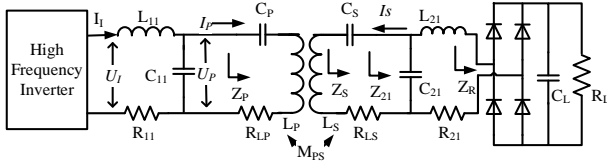


Fig. 2. Wireless power transfer system circuit.

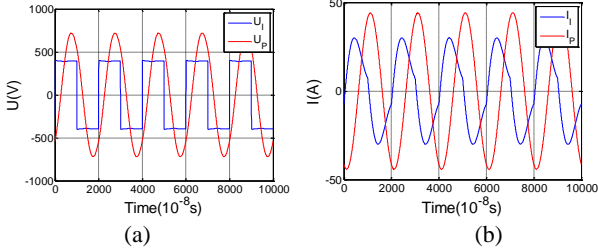


Fig. 3. Voltage and current waves of the primary side: (a) voltage; (b) current.

impedance matching circuit and rectifier load.

As Fig. 2 shows, L_p and L_s are the self-inductances of the primary and secondary coil, respectively, and R_{LP} and R_{LS} are their parasitic resistance. The rectifier load Z_R contains four diodes, a filter capacitance and a resistance. The input voltage of the high frequency inverter is always limited in the design, and the output power is determined by its equivalent load impedance. By using the LCCL topology, the designation of the system parameters can be decoupled. That is to say, a primary impedance matching circuit that includes L_{11} , C_{11} , C_p and L_p , is usually adopted to meet the output power needs of regulating the impedance, while a secondary side impedance that includes L_{21} , C_{21} , C_s and L_s , is used to achieve the maximum transfer efficiency by translating the rectifier load impedance into the optimum load [29], [30].

B. Power Transfer Analysis of the Primary Side

In the wireless power transfer system shown in Fig. 2, the current and voltage of the primary side of the coils are I_p and U_p , while the output current and voltage of the inverter are I_i and U_i . The wave form of U_i is a square wave, while the voltage across capacitor C_{11} , U_p is nearly a sine wave, as is shown in Fig. 3(a). In addition, the current through the capacitor C_p , I_p is much closer to a sine wave than I_i , as is shown in Fig. 3(b). Further calculation has shown that a 2%-3% error is involved when the complex impedance is calculated with U_i and I_i due to the impact of harmonic components. Therefore, for the LCCL topology shown in Fig. 2, the measurement and analysis below are based on U_p and I_p for the sake of convenience and accuracy.

The effective values of I_p and U_p are I_{prms} and U_{prms} , respectively, which can be calculated with the following equations.

$$I_{prms} = \sqrt{\frac{1}{NT} \int_0^{NT} i_p^2(t) dt} \quad (1)$$

$$U_{prms} = \sqrt{\frac{1}{NT} \int_0^{NT} u_p^2(t) dt} \quad (2)$$

where T is the cycle, $i_p(t)$ and $u_p(t)$ are the instantaneous values of I_p and U_p , respectively, and N is the cycle number.

Then, the input active power P_p of the WPT system can be determined in (3), the apparent power S_p of the WPT system can be determined in (4), and the reactive power Q_p is determined in (5).

$$P_p = \frac{1}{NT} \int_0^{NT} i_p(t) u_p(t) dt \quad (3)$$

$$S_p = \frac{1}{NT} \sqrt{\int_0^{NT} i_p^2(t) dt \int_0^{NT} u_p^2(t) dt} \quad (4)$$

$$Q_p = \sqrt{S_p^2 - P_p^2} \quad (5)$$

As shown in Fig.2, Z_p is the quotient of U_p and I_p , and it is assumed that its real part and imaginary part are R_p and X_p . According to circuit theory, equations (6) and (7) should be satisfied.

$$R_p = P_p / I_{prms}^2 \quad (6)$$

$$|X_p| = Q_p / I_{prms}^2 \quad (7)$$

From the above analysis, it can be concluded that the calculation of Z_p is based on the theory of the apparent power S_p , the input active power P_p , and the reactive power Q_p , which can also be used in the calculation of Z_p in systems with different impedance matching topologies such as an LC circuit [23] and an LCL circuit [22].

C. Reflected Impedance Analysis

First, the transfer model for a wireless power transfer system can be described by (8):

$$\begin{bmatrix} U_p \\ 0 \end{bmatrix} = \begin{bmatrix} j\omega L_p + R_{LP} + 1/(j\omega C_p) & j\omega M_{ps} \\ j\omega M_{ps} & Z_s \end{bmatrix} \begin{bmatrix} I_p \\ I_s \end{bmatrix} \quad (8)$$

where Z_s is the equivalent impedance of the secondary loop circuit, and:

$$Z_s = R_{LS} + j(\omega L_s - \frac{1}{\omega C_s}) + Z_{21} \quad (9)$$

It is assumed that R_s is the real part of Z_s , and that X_s is the imaginary part of Z_s . Then, the reflected impedance Z_{sp} , which is the impedance reflected to the primary side from the secondary side, can be described by (10):

$$Z_{sp} = \frac{(\omega M_{ps})^2}{R_s^2 + X_s^2} R_s - j \frac{(\omega M_{ps})^2}{R_s^2 + X_s^2} X_s \quad (10)$$

It is assumed that R_{sp} is the real part of Z_{sp} , and that X_{sp} is the imaginary part of Z_{sp} . It addition, it is assumed that:

$$R_{sp} = \frac{(\omega M_{ps})^2}{R_s^2 + X_s^2} R_s \quad (11)$$

$$X_{sp} = -\frac{(\omega M_{ps})^2}{R_s^2 + X_s^2} X_s \quad (12)$$

TABLE I
SYSTEM PARAMETERS OF THE ESTABLISHED WIRELESS
POWER TRANSFER SYSTEM

Parameter	Value	Parameter	Value
<i>Distance</i>	20cm	<i>Frequency</i>	50kHz
L_P	164.26 μH	L_S	165.69 μH
R_P	0.101 Ω	R_S	0.129 Ω
L_{11}	89.58 μH	C_{11}	174.72 nF
C_P	99.55 nF	C_S	117.7 nF
C_{21}	162.5 nF	L_{21}	86.2 μH
R_{11}	0.067 Ω	R_{21}	0.063 Ω
C_L	3 μF	<i>Input voltage</i>	300V

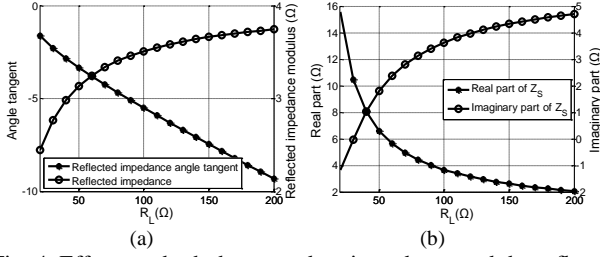


Fig. 4. Effects on both the secondary impedance and the reflected impedance by the RL: (a) reflected impedance; (b) secondary impedance.

The variable λ is used to represent the tangent value of the reflected impedance angle θ . Then:

$$\lambda = X_{SP} / R_{SP} \quad (13)$$

According to equations (11)-(13), λ is described as:

$$\lambda = -X_S / R_S \quad (14)$$

which is unrelated to the mutual inductance M_{PS} , and only related to the secondary loop impedance.

III. PROPOSED ONLINE DETECTION

A. Load Estimation with the Curve Fitting Method

The key to the proposed parameter estimation method is the parameter λ , which is explained in (14). To explore its relationship with R_L , a model of a WPT system as depicted in Fig.2 is built in the Matlab/Simulink environment, and the parameters of the model are shown in Table I.

From the simulation, the relationship between the reflected impedance angle tangent λ and R_L is shown in Fig. 4(a), and the value varies monotonically, which means that R_L can be determined if λ is known. Therefore, it is possible to further determine the secondary side impedance Z_S by exploring the relationship between R_L and Z_S , which is presented in Fig. 4(b).

Because of the nonlinear characteristics of the rectifier load, the relationship between R_L and the secondary loop impedance cannot be derived by the analytical method. The polynomial fitting method is used to determine the function relation between R_L and λ , R_S and λ , and X_S and λ . Fig. 5 shows the fitting process of the parameters. The fitting results are shown in (15)-(17).

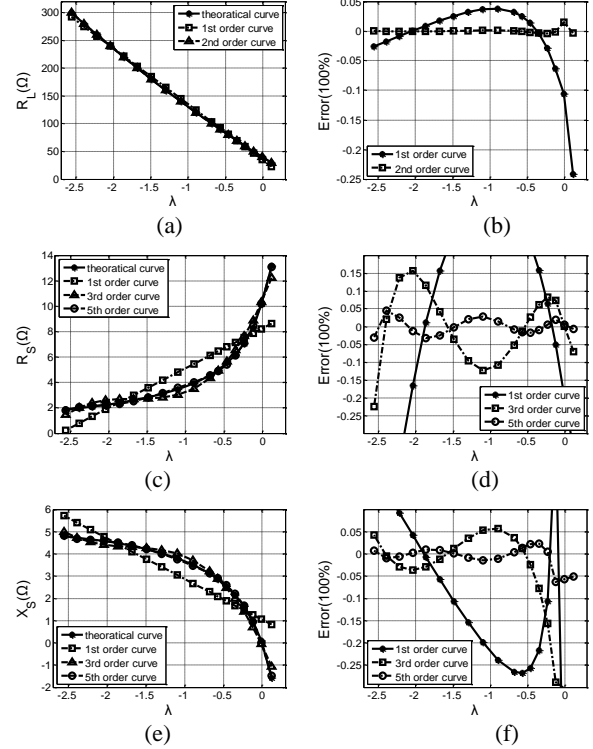


Fig. 5. Curve fitting and error analysis of the parameters: (a)(b) R_L and λ ; (c)(d) R_S and λ ; (e)(f) X_S and λ .

$$R_L = 7.0370\lambda^2 - 83.6746\lambda + 39.7622 \quad (15)$$

$$X_S = -0.4255\lambda^5 - 3.1564\lambda^4 - 8.934\lambda^3 - 12.4788\lambda^2 - 10.0051\lambda - 0.1027 \quad (16)$$

$$R_S = 0.8378\lambda^5 + 6.2732\lambda^4 + 17.8900\lambda^3 + 24.879\lambda^2 + 19.067\lambda + 10.4104 \quad (17)$$

B. Parameter Estimation Theoretical Analysis

Based on the analysis of the reflected impedance in II, the equivalent impedance Z_p in the primary side can be calculated in (18), and the real part R_p and the imaginary part X_p can be derived in (19) and (20).

$$Z_p = j\omega L_p + \frac{1}{j\omega C_p} + R_{LP} + Z_{SP} \quad (18)$$

$$R_p = R_{LP} + \frac{(\omega M_{ps})^2}{R_S^2 + X_S^2} R_S \quad (19)$$

$$X_p = \omega L_p - \frac{1}{\omega C_p} - \frac{(\omega M_{ps})^2}{R_S^2 + X_S^2} X_S \quad (20)$$

According to (19) and (20), λ can be calculated by R_p and X_p in (21):

$$\lambda = -\frac{X_S}{R_S} = \frac{X_p - \omega L_p + 1/(\omega C_p)}{R_p - R_{LP}} \quad (21)$$

Then, it is possible to obtain the mutual inductance M_{PS} in (22) according to (19):

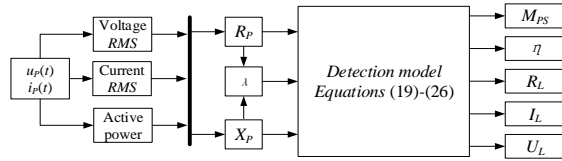


Fig. 6. Detection method diagram for a wireless power transfer system.

$$(\omega M_{ps})^2 = R_S (R_p - R_{Lp})(1 + \lambda^2) \quad (22)$$

Furthermore, the transfer efficiency η is also calculated [31] [32] by (23).

$$\eta = \frac{(R_S - R_{LS})(R_p - R_{Lp})}{R_S R_p} \quad (23)$$

From the above analysis, it can be seen that when λ and Z_S are determined, the parameters M_{PS} and η can also be calculated.

P_T is used to represent the power loss of the secondary impedance matching circuit and rectifier circuit, then the load power, voltage and current are calculated by (24)-(26).

$$P_L = \eta P_p - P_T \quad (24)$$

$$I_L = (P_L / R_L)^{1/2} \quad (25)$$

$$U_L = (P_L R_L)^{1/2} \quad (26)$$

C. Load Detection Model

The proposed detection model can be described by Fig. 6. Through the reflected impedance calculation, many of the load parameters can be estimated by the detection model, such as R_L , M_{PS} , η , I_L and U_L , which are important for the online control of wireless power transfer systems.

IV. SIMULATION AND EXPERIMENT VERIFICATION

A wireless power transfer system is established to efficiently transfer a power of 3kW over a distance of 22cm with the circuit shown in Fig. 2, and the system elements values are listed in Table. I. In this system, a primary *LCCL* impedance matching circuit is used to meet the power needs, and a secondary *LCCL* impedance matching circuit is used to satisfy the maximum transfer efficiency at the rate of the output power operating state.

A. Dynamic Simulation of Load Detection

A simulation model is built with Matlab/Simulink tools to verify the proposed load detection method. The proposed load detection method is dynamically applied in the simulation model, and the simulation results are shown in Fig. 7, where (a) is the variation of R_L , (b) is the load current, (c) is the square of the product of the angular frequency of the system and the mutual inductance between coils, and (d) is the system efficiency. It can be observed from the pictures that the estimated values can reach the stable state within 1ms.

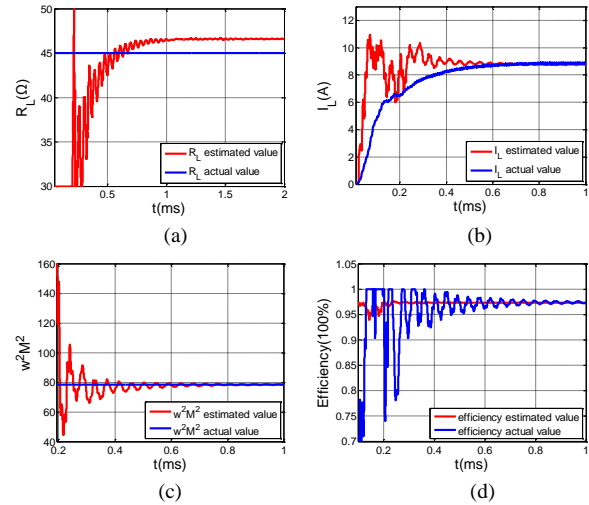


Fig. 7. Dynamic simulation results of load detection.

B. Load Detection Hardware Design

In order to further verify the proposed parameter estimation method, a WPT experiment system has been designed. The values of the system elements are listed in Table. I. Fig. 8 shows some photographs of the three parts of the established system: (a) the resonant coils; (b) the primary side; and (c) the secondary side. In Fig. 8(a), magnetic disks made of ferrites are added to improve the power transfer efficiency, and the coils are made of Litz line. In Fig. 8(b), the DC/AC inverter is a voltage-fed inverter driven by 4 high frequency pulses. In Fig. 8(c), a full-wave bridge rectifier is used as a AC/DC converter.

In a wireless power transfer system, a high sampling rate is needed to improve the precision for equivalent impedance calculating in the primary side. A FPGA processor EP2C8Q208I8 is used to realize the load detection method, which can work at a frequency of 50MHz. The real-time signals of $u_p(t)$ and $i_p(t)$ are measured by sensors, and then translated into digital data by the AD unit. The voltage sensor is a Yubo CHV-25P with a response time of 10 μ s and a measurement bandwidth of 0-100kHz. The current sensor is a LA55-P/SP50 produced by LEM Company, with a response time of 1 μ s and a measurement bandwidth of 0-200kHz. An ADC9218 is used as the AD unit, with 10 independent A/D converters and a converting speed of 105MSPS. The load detection unit obtains digital data from the AD unit using parallel data communication, and it calculates the parameters R_L , M_{PS} , η , I_L and U_L . The system information is digitally displayed by the LED in the signal indication unit. Fig. 9 is the proposed online parameter load detection circuit, and the hardware of the load detection system shown in Fig. 11, where (a) is the sensor circuit, and (b) is the FPGA processor.

C. Parameter Estimation Results

An experiment was conducted with the WPT experimental system designed in part B. A series of values for R_L and M_{PS} was sampled to estimate with the proposed method. The

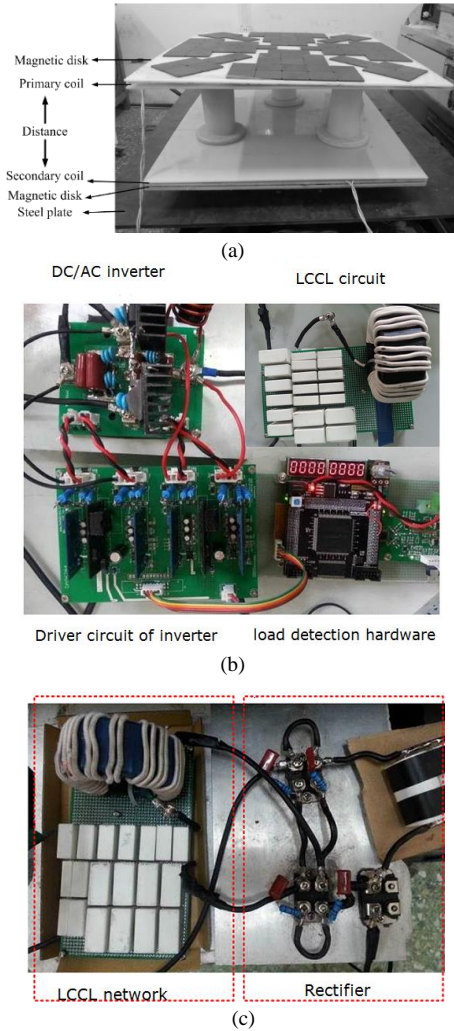


Fig. 8. Three parts of the wireless power transfer system: (a) resonant coils; (b) primary side; (c) secondary side.

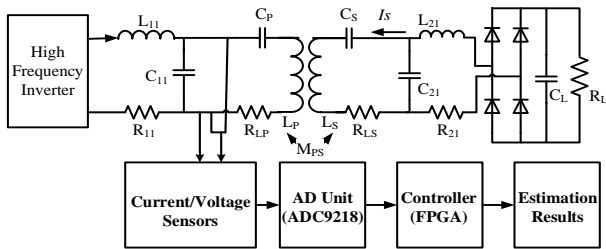


Fig. 9. Online parameter estimation circuit.

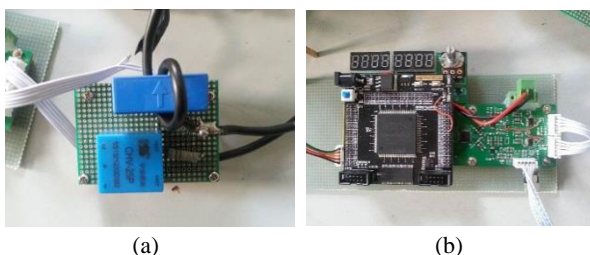


Fig. 10. Photograph of the load detection hardware: (a) the sensor circuit; (b) the FPGA processor.

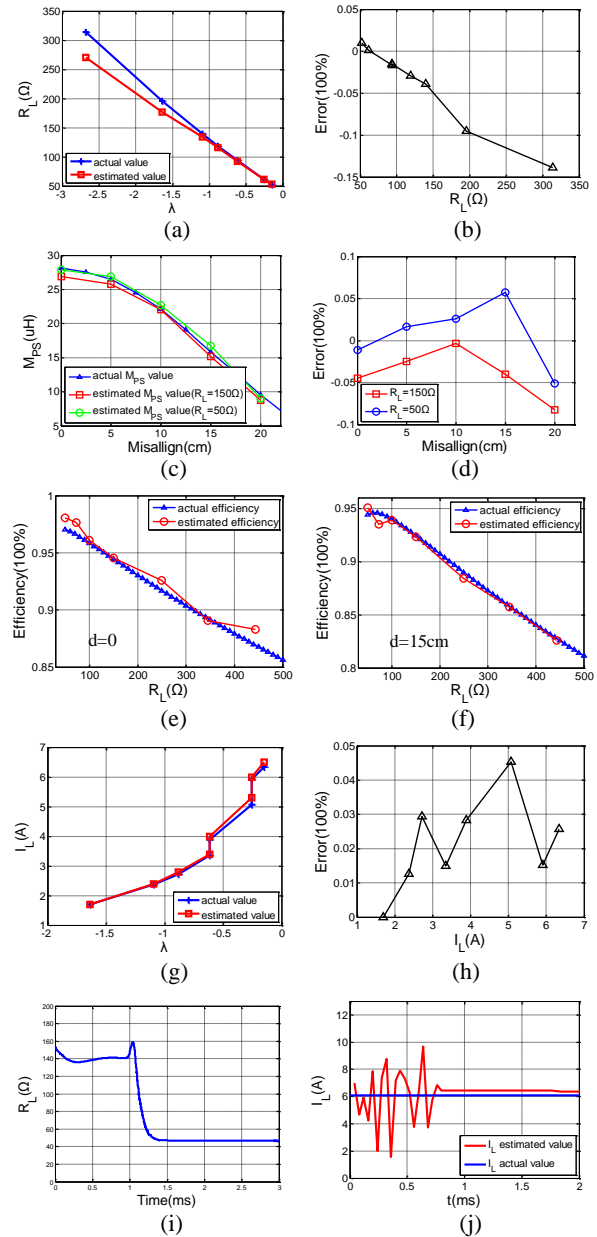


Fig. 11. Experiment results of load the detection.

results of the experiment are shown in Fig. 11, where (a) describes the λ - R_L relation, and Fig. 11(b) describes the error of the estimated value of R_L . The estimation error can be kept under 10% when the resistance load is less than 200Ω . Fig. 11 (c) and (d) describe the estimated M_{PS} value and errors under different resistance loads, and the error can be controlled to within 5% considering that the misalign distance of the coils is generally less than 15cm. Fig. 11(e) and (f) show the estimated system efficiency under different coils misalign distances (0cm and 15cm, respectively) in the circumstance when $R_L=45\Omega$. In addition, Fig. 11(g) and (h) describe the estimated value and error of I_L and its error when $R_L=45\Omega$. From this result it can be seen that when the load is charged with a 1-7A current, the estimated error of I_L can be controlled to under 5%.

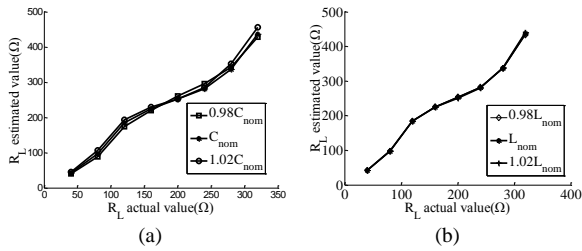


Fig. 12. Sensitivity to system parameters of the proposed estimation method.

To verify the dynamic characteristics of the proposed parameter estimation method, dynamic experiments were carried out and the results are shown in Fig. 11(i) and (j). In Fig. 11(i), when the load changes from 140Ω to 45Ω at 1ms, the estimation result of R_L falls rapidly and reaches its steady state within 0.5ms. In Fig. 11(j), when the input voltage changes, the estimated value of I_L can eliminate the interference within 0.5ms.

Both the simulation and the experimental results show the accuracy and reliability of the proposed parameter estimating method. The dynamic response characteristics of the method are verified with both simulation and experimental results and all of the parameters can reach the stable state within 1ms, where the response time of I_L is within 0.6ms. In addition, the accuracy of the method is verified with experiments. It has been shown that when the misalign distance is lower than 15cm and the equivalent resistance load R_L is less than 200Ω, high estimating accuracy can be guaranteed.

D. Sensitivity Analysis of the Proposed Estimation Method

The proposed parameter estimation method is based on the curve fitting method. The curve fitting results are dependent on system parameters such as C_{21} , L_{21} and so on. However, the values of the system parameters may change due to variant environmental temperatures, external electromagnetic interference and other unpredictable factors. Therefore, it is necessary to perform sensitivity analysis on the system parameters.

In Fig. 12, the estimated values of R_L under different values of C_{21} and L_{21} are analyzed. It is assumed that the values of C_{21} and L_{21} listed in Table 1 are the nominal values of the system, and that they are represented with C_{nom} and L_{nom} . An $\pm 2\%$ error of the capacitors and inductors is taken into consideration during the operation process of the system.

Fig. 12(a) shows that with variations of C_{21} , there are fluctuations of the estimated values of R_L , which are in a normal range of estimation errors. Fig. 12 (b) shows that with variations of L_{21} , there are nearly no variations of the estimated value of R_L . It can be seen from Fig. 7 that changes of C_{21} have a greater impact on the parameters that need to be estimated than L_{21} .

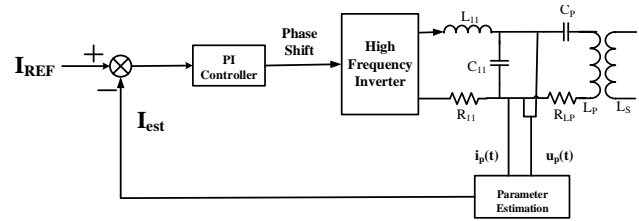


Fig. 13. Single controller of a WPT system.

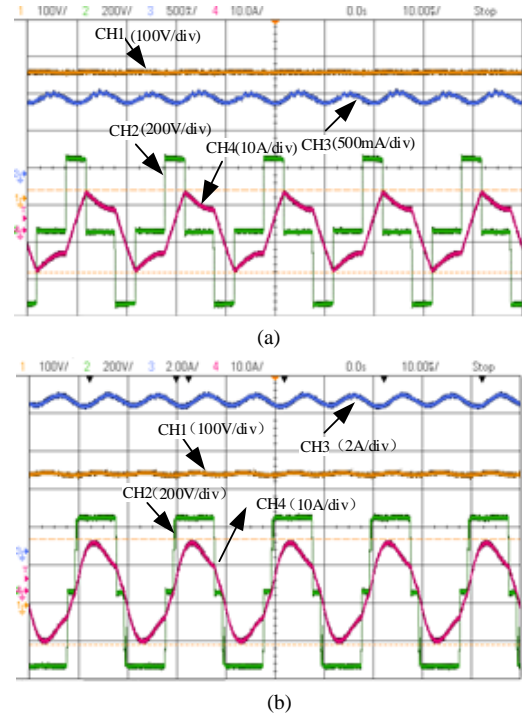


Fig. 14. Experiment results of the load current control (CH1: load voltage; CH2: output voltage of the inverter; CH3: load current; CH4: output current of the inverter).

V. APPLICATION OF THE PROPOSED DETECTION

To demonstrate the practicality of the proposed online parameter estimation method for WPT systems, a single controller in the primary side is proposed to achieve constant current control.

As shown in Fig. 13, the estimated load current I_{est} is compared with the reference current I_{REF} . Then, a PI controller is used to achieve phase shift control over the high frequency inverter.

A set of lead-acid battery packs with a nominal voltage of 340V is chosen as the load of the WPT system and is tested with the proposed control method. Reference currents of 1A and 8A are assigned to the load detection and control system, respectively. When the control target is 1A, the phase shift angle of the inverter is 104° , and the average value of the actual load current is 1.022A with an error of 2.2%, as shown in Fig. 14(a). When the control target is 8A, the average value of the actual load current is 7.98A with an error of 0.25%, as shown in Fig. 14(b).

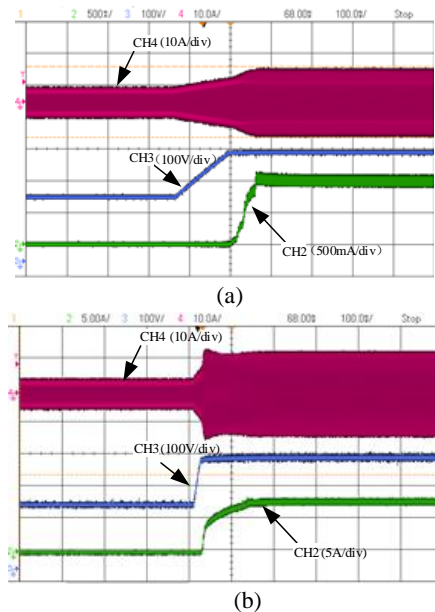


Fig. 15. Transient experiment results of the load current control (CH2: load current; CH3: load voltage; CH4: output current of the inverter).

The transient response of the proposed control strategy is verified by a series of experiments. Before charging, the system works under the no-load condition, with an output voltage of 200V. When the control objective is set to 1A, the load voltage rises from 200V to 340V in 150ms, and the load current rises from 0A to 1A in 70ms, as shown in Fig. 15 (a). The regulation time of the output current of the inverter is about 200ms. In Fig. 15(b), the control objective is set to 8A. The load voltage rises from 200V to 340V in 30ms, the load current rises from 0A to 1A in 100ms, and the regulation time of the output current of the inverter is about 150ms.

VI. CONCLUSIONS

In this paper, a parameter estimation method for wireless power transfer systems using the tangent of the reflected impedance angle is introduced. The resistance load, output power, output efficiency, load current and mutual inductance of the coils can be estimated by measuring the primary side voltage and current with this method. The dynamic response characteristics of the method are simulated and all of the parameters can reach the stable state within 1ms. In addition, for most working conditions of the wireless power transfer system, the estimation error of the load can be less than 10%, and the estimation error of the charging current can be less than 5%. A single controller based on the proposed parameter estimation method is established. It is capable of achieving constant current control with a high response rate.

The theoretical analysis in this paper avoids the influence of coils misalignment with the introduction of the tangent value of the reflected impedance angle λ . Then, it estimates the secondary loop parameters with the polynomial fitting

method, and realizes the online estimation of the resistance load and coils mutual inductance. The estimation results show that this method basically meets the needs for estimating accuracy, and it can be used in the single controller strategy of wireless power transfer systems. With such methods, information of the primary side instead of the receiving terminal is collected. Then, the equivalent load and charging current are estimated, providing controlling information for the single controller on the primary side. This controlling strategy removes both the receiving terminal controller and the wireless communication, improving the reliability of the system while reducing its costs and size. The controlling strategy can be applied in a wide range of fields involving WPT systems, including electrical vehicles, mobile devices and so on.

ACKNOWLEDGMENT

This work is financially supported by National High Technology Research and Development Program of China (2015AA016202).

REFERENCES

- [1] S. Y. Hui, "Planar wireless charging technology for portable electronic products and Qi," in *Proc. IEEE*, Vol. 101, No. 6, pp. 1290-1301, Jun. 2013.
- [2] U. K. Madawala and D. J. Thrimawithana, "A bidirectional inductive power interface for electric vehicles in V2G systems," *IEEE Trans. Ind. Electron.*, Vol. 58, No. 10, pp. 4789-4796, Oct. 2011.
- [3] P. Si, A.P. Hu, S. Malpas, and D. Budgett, "A frequency control method for regulating wireless power to implantable devices," *IEEE Trans. Biomed. Circuits Syst.*, Vol. 2, No. 1, pp. 22-29, Mar. 2008.
- [4] J. Shin, S. Shin, Y. Kim, S. Ahn, S. Lee, G. Jung, S. Jeon, and D. Cho, "Design and implementation of shaped magnetic-resonance-based wireless power transfer system for roadway-powered moving electric vehicles," *IEEE Trans. Ind. Electron.*, Vol. 61, No. 3, pp. 1179-1192, Mar. 2014.
- [5] Q. Li and Y.C. Liang, "An inductive power transfer system with a high-Q resonant tank for mobile device charging," *IEEE Trans. Power Electron.*, Vol. 30, No. 11, pp. 6203-6212, Nov. 2015.
- [6] C. Wang, O. H. Stielau, and G. A. Covic, "Design considerations for a contactless electric vehicle battery charger," *IEEE Trans. Ind. Electron.*, Vol. 52, No. 5, pp. 1308-1314, Oct. 2005.
- [7] J. Sallan, J. L. Villa, A. Llombart, and J. F. Sanz, "Optimal design of ICPT systems applied to electric vehicle battery charge," *IEEE Trans. Ind. Electron.*, Vol. 56, No. 6, pp. 2140-2149, Jun. 2009.
- [8] D. Ahn and S. Hong, "Effect of coupling between multiple transmitters or multiple receivers on wireless power transfer," *IEEE Trans. Ind. Electron.*, Vol. 60, No. 7, pp. 2602-2613, Jul. 2013.
- [9] T. Beh, M. Kato, T. Imura, S. Oh, and Y. Hori, "Automated impedance matching system for robust wireless power transfer via magnetic resonance coupling," *IEEE Trans. Ind. Electron.*, Vol. 60, No. 9, pp. 3689-3698, Sep. 2013.
- [10] S. Iguchi, P. Yeon, H. Fuketa, K. Ishida, T. Sakurai, and M. Takamiya, "Wireless power transfer with zero-phase-difference capacitance control," *IEEE Trans. Circuits Syst. I*,

- Reg. Papers*, Vol.62, No. 4, pp. 938-947, Apr. 2015.
- [11] W. Zhong and S.Y.R. Hui, "Auxiliary circuits for power flow control in multifrequency wireless power transfer systems with multiple receivers," *IEEE Trans. Power Electron.*, Vol. 30, No. 10, pp. 5902-5910, Oct. 2015.
- [12] J. Lee, B. Lee, S. Lee, and K. Yi, "A study on the control of output current to respond to the load changes of the wireless power transfer," *IEEE Transportation Electrification Conference and Expo (ITEC)*, pp. 1-4, 2015.
- [13] J.T. Boys, C.-Y. Huang, and G.A. Covic, "Single-phase unity power-factor inductive power transfer system," *IEEE Power Electronics Specialists Conference*, pp. 3701-3706, 2008.
- [14] H. L. Li, A. P. Hu, G. A. Covic, and C. Tang, "A new primary power regulation method for contactless power transfer," *IEEE International Conference on Industrial Technology*, pp. 1-5, 2009.
- [15] N.Y. Kim, K.Y. Kim, J. Choi, and C. Kim, "Adaptive frequency with power-level tracking system for efficient magnetic resonance wireless power transfer," *Electronics Lett.*, Vol. 48, No. 8, pp. 452-454, Apr. 2012.
- [16] A. P. Hu and H. S., "Improved power flow control for contactless moving sensor applications," *IEEE Power Electronics Lett.*, Vol.2, pp. 135-138, Dec. 2004.
- [17] G. Chen, Y. Sun, X. Dai, and Z. Wang, "On piecewise control method of Contactless Power Transmission system," in *Proceedings of the Control Conference*, pp. 72-75, 2008.
- [18] T. Diekhans and R.W. De Doncker, "A dual-side controlled inductive power transfer system optimized for large coupling factor variations and partial load," *IEEE Trans. Power Electron.*, Vol. 30, No. 11, pp. 6320-6328, Nov. 2015.
- [19] J. Yin, D. Lin, C. K. Lee, and S. Y. R. Hui, "Load monitoring and output power control of a wireless power transfer system without any wireless communication feedback," in *Proc. IEEE Energy Convers. Congr. Expo.*, pp. 4934-4939, 2013.
- [20] U. K. Madawala, M. Neath, and D. J. Thrimawithana, "A power-frequency controller for bidirectional inductive power transfer system," *IEEE Trans. Ind. Electron.*, Vol. 60, No. 1, pp. 310-317, Jan. 2013.
- [21] G. R. Nagendra, L. Chen, G. A. Covic, and J. T. Boys, "Detection of EVs on IPT highways," in *Proc. 29th Annu. IEEE Applied Power Electronics Conference and Exposition*, pp. 1604-1611, 2014.
- [22] U. K. Madawala and D. J. Thrimawithana, "A single controller for inductive power transfer systems," in *Proc. IEEE Ind. Electron. Conf.*, pp. 109-113, 2009.
- [23] Z. H. Wang, Y. Li, Y. Sun, C. Tang, and X. Lv, "Load Detection Model of Voltage-Fed Inductive Power Transfer System," *IEEE Trans. Power Electron.*, Vol. 28, No. 11, pp. 5233-5243, Nov. 2013
- [24] Y. P. Su, L. Xun, and S. Y. R. Hui, "Mutual inductance calculation of movable planar coils on parallel surfaces," in *IEEE Power Electronics Specialists Conference*, pp. 3475-3481, 2008.
- [25] J. Yin, D. Lin, C. Lee, S.Y.R. Hui, "A systematic approach for load monitoring and power control in wireless power transfer systems without any direct output measurement," *IEEE Trans. Power Electron.*, Vol. 30, No. 3, pp. 1657-1667, Mar. 2015.
- [26] J. L. Villa, J. F. Osorio, and A. Llombart, "High-misalignment tolerant compensation topology for ICPT systems," *IEEE Trans. Ind. Electron.*, Vol. 59, No. 2, pp. 945-951, Feb. 2012.
- [27] T. Imura and Y. Hori, "Maximizing air gap and efficiency of magnetic resonant coupling for wireless power transfer using equivalent circuit and neumann formula," *IEEE Trans. Ind. Electron.*, Vol. 58, No. 10, pp. 4746-4752, Oct. 2011.
- [28] Y. P. Su, X. Liu, and S. Y. R. Hui, "Mutual inductance calculation of movable planar coils on parallel surfaces," *IEEE Trans. Ind. Electron.*, Vol. 24, No. 4, pp. 1115-1124, Apr. 2009.
- [29] J. J. Casanova, Z. Low, and J. Lin, "A loosely coupled planar wireless power system for multiple receivers," *IEEE Trans. Ind. Electron.*, Vol. 56, No. 8, pp. 3060-3068, Aug. 2009.
- [30] L. Chen, S. Liu, Y. Zhou, and T. Cui, "An optimizable circuit structure for high-efficiency wireless power transfer," *IEEE Trans. Ind. Electron.*, Vol. 60, No. 1, pp. 339-349, Jan. 2013.
- [31] M. Pinuela, D. C. Yates, S. Lucyszyn, and P. D. Mitcheson, "Maximizing DC-to-load efficiency for inductive power transfer," *IEEE Trans. Power Electron.*, Vol. 28, No. 5, pp. 2437-2447, May. 2013.
- [32] M. Fu, T. Zhang, C. Ma, and X. Zhu, "Efficiency and optimal loads analysis for multiple-receiver wireless power transfer systems," *IEEE Trans. Microw. Theory Techn.*, Vol. 63, No. 3, pp. 801-812, Mar. 2015.



Shufan Li received his B.S. degree from the Beijing Technology and Business University, Beijing, China, in 2013; his M.S. degree at the University of Chinese Academy of Sciences, Beijing, China, in 2016, where he is presently working towards his Ph.D. degree in Power Electronics and Electric Drives. His current research interests include wireless power transfer theory, parameter estimation and the control of wireless charging systems.



Chenglin Liao received his Ph.D. degree in Power Machinery and Engineering from the Beijing Institute of Technology, Beijing, China, in 2001. After that, he had spent two years as a Postdoctoral Researcher at Tsinghua University, Beijing, China. He is presently working as the Deputy Director of the Department of Vehicle Energy System and Control Technology, Institute of Electrical Engineering, Chinese Academy of Sciences, Beijing, China, where he had been involved in research on battery management systems, vehicle control and wireless charging systems for electric vehicles for the past nine years. His current research interests include the development of high power wireless charging systems for commercial Electric Vehicles.



Lifang Wang received her Ph.D. degree from Jilin University, Changchun, China, in 1997. After that, she joined the Institute of Electrical Engineering (IEE), Chinese Academy of Sciences, Beijing, China. During the Chinese tenth-five year plan (2001-2005), she was a Member of the national specialist group of the Key Special Electric Vehicle Project of the National 863 Program, and she was the Head of the 863 Special EV Project Office. She is presently working as the Director of the Department of Vehicle Energy Systems and Control Technology at IEE. She is also the Vice Director of the Key Laboratory of Power Electronics and Electric Drives, Chinese Academy of Sciences. Her current research interests include Electric Vehicle control systems, EV battery management systems, wireless charging systems for EVs, electromagnetic compatibility and smart electricity use. She has directed more than 15 projects, published more than 50 papers and has 25 patents in these fields.